Iraqi Journal of Computers, Communications, Control and Systems Engineering
Journal homepage: https://ijccce.uotechnology.edu.iq

Flatness-Based Active Disturbance Rejection Control with B-Spline Output Regulation for a Chemical Reactor

Qasim M. Hamad[1,*], Safanah M. Raafat[2]

[1]Electrical Engineering Department, University of Babylon, Babil, Iraq.
[2]Control and System Engineering College, University of Technology, Baghdad, Iraq.
[1]kasimalhussani@uobabylon.edu.iq ,[2]safanah.m.raafat@uotechnology.edu.iq

DOI: https://doi.org/10.33103/uot.ijccce.25.2.1

HIGHLIGHTS

- A 2DOF control strategy was developed using differential flatness for feedforward and feedback control of a nonlinear CSTR system.
- A disturbance observer was integrated with the feedback controller to form a Flatness Active Disturbance Rejection Control (FADRC) scheme.
- B-spline curves generated reference trajectories that symbolically handle state and input constraints.
- The B-spline-based trajectory was compared with a switching function-based trajectory to assess tracking, smoothness, and disturbance robustness.

ARTICLE HISTORY

Received: 16/ February /2025

Revised: 24/ April /2025

Accepted: 09/ May /2025

Available online: 30/ October /2025

Keywords:
Flatness Control, Active disturbance rejection control, trajectory design, B-

ABSTRACT

Model uncertainties and exogenous disturbances are inherent phenomena in chemical plants that degrade performance and lead to poor-quality products. To mitigate these issues, this paper addresses disturbances by exploiting the differential flatness property (DFP) of the nonlinear continuous stirred tank reactor (NCSTR). A two-degree-of-freedom (2DOF) control design was implemented, incorporating flatness-based feedforward and feedback controllers. This design leverages the differential flatness method for effective stabilization and tracking performance. A robust feedback tracking control strategy integrating a disturbance observer (DO) and a simple feedback controller was implemented to form a flatness active disturbance rejection control (FADRC) scheme. The B-spline technique was used for trajectory generation to enhance the performance of the proposed control strategy. Additionally, constraints were handled symbolically rather than numerically by designing B-spline curves for the system's flat output. This approach ensures a feasible open-loop reference trajectory that satisfies the feedback controller's states and input constraints. A comparison was conducted between the switching function-based (SF) trajectory and the B-spline (Bs) designed reference trajectory regarding their impact on system tracking performance, smoothness, and robustness to disturbances. A detailed analysis evaluated tracking

spline .

errors, control effort, and disturbance rejection capabilities under both trajectory designs. The proposed flatness-based ADRC methodology efficiently managed exogenous disturbances and constraints on the input of a nonlinear plant.

I. INTRODUCTION

Disturbances in chemical processes are unavoidable and stem from variations in the inlet concentration and temperature of the raw materials. Moreover, other sources of disturbances contribute to instability and performance degradation, such as environmental conditions, sensor noise, and equipment performance. Countless innovative control techniques have been suggested to control chemical processes [1],[2]. In [3] and [4], evolutionary algorithms have been used to control and optimize chemical reactors. SMC [5],[6] demonstrates excellent control of various chemical systems, including continuous stirred tank reactors and mixing tanks. Model Predictive Control (MPC) is a standard for controlling multivariable industrial processes in chemical and refining industries [7]. Recent advancements in MPC include machine learning-aided approaches [8], incorporating multi-objective optimization and multi-criteria decision-making, demonstrating improved performance in complex chemicals.

Recent studies concerning disturbances in chemical processes and reactors have focused on advanced control strategies. In [9], machine learning-based predictive control structures have been developed for nonlinear processes, combining recurrent neural networks (RNN) with Lyapunov-based model predictive controllers to deal with bounded and stochastic disturbances. An enhanced automatic disturbance rejection control method has been proposed in [10]. For CSTR, it enhances confrontation with external disturbances and reduces parameter sensitivity. An improved 2DOF robust PID control law has been calculated for various chemical processes, ensuring satisfactory performance for step and ramp-type references and disturbances [11]. Additionally, additive and multiplicative feedforward control structures have been assessed in [12], evaluating their effectiveness in improving closed-loop dynamic responses to load disturbances in distillation columns and reactors. In [13], an enhanced dual-DOF PI-PD control for chemical processes was designed using rigorous perturbation analysis. These advancements aim to improve process control and disturbance rejection in chemical systems.

Active Disturbance Rejection Control (ADRC) is a promising technique [14] that emerged for controlling various systems [15], including chemical processes. When combined with soft sensors and U-model control, ADRC demonstrates improved robustness and reduced phase delay in dissolved oxygen regulation for wastewater treatment [16]. A quantitative tuning method for ADRC has been developed for high-order processes, showing superior performance compared to PID control strategies in various applications, including superheater steam temperature control [17]. ADRC's data-driven nature has led to its successful implementation in manufacturing, process control, robotic systems, and energy systems, with major companies recognizing it as an effective alternative to PID control [18].

Furthermore, an equivalence between Extended State Observer-based ADRC and Flat Filter controllers has been established for perturbed pure integration systems, which are paradigmatic for SISO flat nonlinear systems. This equivalence has practical applications in designing Flat Filter controllers for linear control of nonlinear flat systems [19]. For lower triangular nonlinear systems with mismatched stochastic disturbances, a backstepping ADRC approach using second-order extended state observers has been developed [20]. ADRC has also been applied to uncertain nonholonomic systems, employing a switching strategy and input-state scaling to stabilize the system globally [21]. Furthermore, a novel resonant extended state observer (RESO) has been introduced to address harmonic uncertainties in control-affine systems, offering improved tracking accuracy and disturbance

rejection compared to conventional ADRC solutions [22]. These studies demonstrate the versatility and effectiveness of ADRC in handling various nonlinear systems with uncertainties and disturbances. Disturbance estimator techniques are crucial for improving the performance and robustness of various systems [23],[24],[25]. Recent surveys have explored these methods for marine vehicles [26] and quadrotors [27], highlighting approaches like disturbance observers, extended state observers, and adaptive control techniques. A unified disturbance-estimation-based control framework has been proposed, demonstrating equivalence with internal model control and PID controllers, particularly for DC-DC boost converters [28]. A machine learning-assisted approach has been developed to enhance conventional disturbance observer-based control by updating the nominal model, improving disturbance rejection performance [29]. These techniques estimate and compensate for external disturbances and uncertainties in real time, enhancing system adaptability and robustness across various applications, including marine environments, aerial vehicles, and power electronics.

Recent research on B-spline reference trajectory design focuses on improving accuracy, vibration avoidance, and cooperative driving in various applications. [30] Proposed a repetitive control scheme that modifies B-spline trajectories in real time to compensate for external loads and unmodeled dynamics in industrial robots. [31], developed a method to generate robust trajectories that avoid unwanted vibrations in precision manufacturing equipment using B-splines and frequency spectrum optimization. [32] Presented an algorithm for smooth and collision-free trajectory generation in cluttered environments using cubic B-splines, incorporating a two-layer local adjustment strategy and fast trajectory pruning. In [33], the gap between cooperative vehicle following and trajectory planning was bridged by using B-splines to generate cooperative trajectories for automated vehicles, demonstrating string-stable behavior even under considerable communication delays. These studies highlight the versatility and effectiveness of B-splines in various trajectory design applications. An extended form of the ADRC to a differentially flat system [34] was introduced to form a flatness-based ADRC (FADRC). As described in [35], the flatness property is utilized in designing an observer that can estimate the total disturbances and compensate for their effect using ADRC [36].

The current study aims to apply FADRC to a nonlinear CSTR system to estimate the disturbances imposed by an exogenous input temperature of the supplied feed. In addition, in an attempt to enhance the performance of the system's response, the B-spline trajectory design technique was utilized. The contribution of the paper is summarized as follows:

- The integration of B-spline trajectory design with FADRC has been presented for the CSTR system to enhance the response of the proposed strategy.
- Robustness analysis of the proposed FADRC is evaluated by considering the disturbance of the exogenous temperature feed input.

This paper is organized as follows: Section II demonstrates the modeling of CSTR systems. Section III discusses the background knowledge of the Flatness property and ADRC. The suggested designs and computer simulation results are discussed in sections IV and V, respectively. Finally, the conclusion is given in Section VI.

II. MODEL DESCRIPTION

We consider a nonlinear continuous stirred tank reactor (NCSTR), as shown in *Fig. 1*. The vessel is equipped with an agitator for mixing and a jacket surrounding the tank for heating or cooling. The first-order chemical reaction A→C is composed of two reactants that form a product. The reaction is irreversible, exothermic, and contained in a constant volume vessel. The feed stream enters the vessel, and the exit is the liquid product flow from the bottom. The product stream composition and temperature are precisely the contents of the liquid in the vessel. The latter statement is true under steady-state conditions and dynamically at any process time.

The role of the heat removal system (cooling jacket) is to dissipate heat generated in the reactor to prevent thermal runaway. The latter phenomenon leads to uncontrollable operation and is considered a safety hazard. The reactor temperature must be actively controlled and operated within safe limits to prevent thermal runaway.

The model is defined by two nonlinear differential equations that describe the dynamic evolution of reactant A's concentration and the reactor temperature. Additionally, a third algebraic equation incorporates the Arrhenius-based kinetic equilibrium, which is scaled according to the concentration. The relationship between reactor temperature and the specific reaction rate is sensitive in controlling the reactor temperature thermal behavior and stability, as shown in *Fig. 2*.

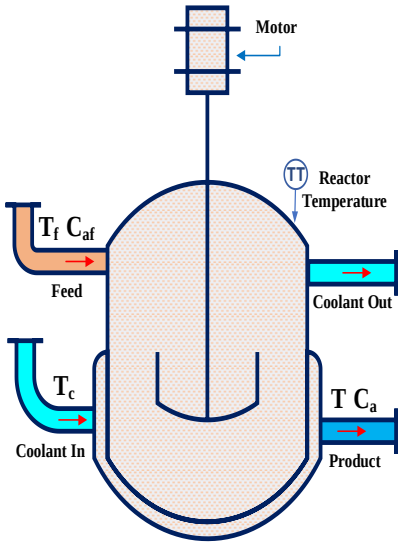

FIG. 1. JACKETED CSTR.

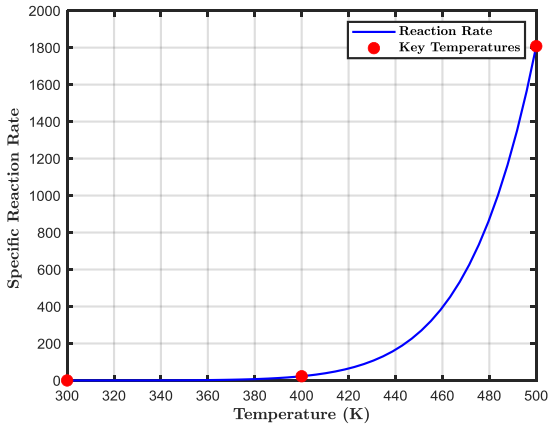

FIG. 2. ARRHENIUS EFFECT.

The nonlinear CSTR model is formulated based on mass balance and energy conservation principles, assuming perfect mixing, negligible heat losses, and a constant reactor volume.

$$\dot{C}_A(t) = \frac{F}{V}\Big(C_{Af} - C_A(t)\Big) - k(T) \tag{1}$$

$$\dot{T}(t) = \frac{F}{V}\Big(T_f - T(t)\Big) + \frac{(-\Delta H)}{\rho C_p}k(T) + \frac{UA}{V\rho C_p}(T_c - T(t)) \tag{2}$$

$$k(T) = k_0 e^{(\frac{-E}{RT(t)})} \mathrm{C}_A(t) \tag{3}$$

The states of the NCSTR model are given by $[\mathrm{C}_A\ T]^T$, while the inputs consist of $[\mathrm{C}_{Af}\ T_f\ T_c]^T$. The reactor concentration and temperature $[\mathrm{C}_A\ T]^T$, represent the system outputs. As shown in Table I, the nominal operating conditions correspond to an unstable equilibrium point. The measured output variable (MO) is the reactor temperature (T), while the reactant concentration (C_A) is an unmeasured output(UO). The manipulated variable (MV) is the jacket coolant temperature (T_c), whereas the feed temperature (T_f) act as a disturbance.

TABLE I. NOMINAL OPERATION VALUES

Parameter	Value	Description
F	100 L/min	Volumetric flow rate
V	100 L	Reactor volume
k0	7.2×10^{10} 1/min	Pre-exponential factor
-ΔH	50000 J/mol	Heat of reaction per mole
E/R	8750 K	Activation energy per mole
Roh	1000 g/L	Density
Cp	0.239 J/g K	Heat capacity
UA	50000 J/min K	Heat transfer coefficient
T_C	300 K	Colling Temperature
C_A	0.5 mol/L	Concentration in the reactor
T	300 K	Reactor temperature

Variations in the feed stream cause fluctuations in the CSTR's outputs, disrupting the process and necessitating an effective control strategy to maintain stable operation. This strategy ensures the reactor follows a specified reference trajectory, enabling smooth and efficient performance.

It is required to design a robust feedback control law to formulate the control problem for the given CSTR Plant, which is modeled by nonlinear differential equations (1-2). This tracking control law must be constructed to force the reactor temperature to follow a desired reference trajectory. The designed controller must act robustly in the face of unknown exogenous disturbance inputs, ignored dynamics, and other unmodeled disturbances. In addition, constraints are imposed on the control signal to ensure feasible operation, restricting it within the range as $250 \leq u \leq 320$ K. It is also required to provide a smooth alternative to the step function while maintaining comparable transition dynamics, enabling a meaningful performance comparison regarding tracking accuracy, control effort, and disturbance rejection.

III. BACKGROUND KNOWLEDGE

A. Differential Flatness for a nonlinear SISO system

Michel Fliess and his coauthors [35] introduced the concept of differential flatness for nonlinear systems. A key property of flat systems is the existence of a finite set of variables, known as flat outputs or linearizing outputs, that fully describe the system's dynamics. To provide a brief overview of differentially flat systems and their fundamental characteristics, we consider a nonlinear system represented by:

$$\dot{x}(\mathrm{t}) = f\big(x(t), u(t)\big) \tag{4}$$

$$y(t) = h(x) \tag{5}$$

with $x(t) \in R^n, u(t) \in R^m, y(t) \in R^m$ and f, h are smooth functions within their respective domains. System (1) is considered differentially flat if there exists a flat output variable ζ that satisfies the following conditions:

1. Flat output ζ can be expressed as a function of the system's state, inputs, and a finite number of their derivatives:

$$\zeta = \psi(x, u, \dot{u}, \dots, u^{(n)}) \tag{6}$$

where ψ is a smooth function and n is the required differentiation order of the input.

2. The system state and input can be expressed in terms of the flat output ζ and a finite number of its derivatives as follows:

$$x = \psi_1(\zeta, \dot{\zeta}, \dots, \zeta^{(n-1)}) \tag{7}$$

$$u = \psi_2(\zeta, \dot{\zeta}, \dots, \zeta^{(n)}) \tag{8}$$

where ψ_1 and ψ_2 are smooth functions and n represents the required differentiation order of the flat output.

3. If the system satisfies these conditions, the actual system output y can be expressed as a function of the flat output ζ and a finite number of its time derivatives:

$$y = \psi_3\left(\zeta, \dot{\zeta}, \dots, \zeta^{(n_y)}\right) \tag{9}$$

where ψ_3 is a smooth function and n_y denotes the required differentiation order of the flat output to describe the system output.

By leveraging the flatness property through the feedforward control law in Eq. (8) and the reference trajectory in Eq. (7), expressed in terms of the flat output and its derivatives, the system variables can be directly obtained as time functions without requiring integration.

Generally, a differentially flat system can be represented using Brunovsky coordinates or flat states, which provide a canonical form where the flat output and its derivatives explicitly parameterize system dynamics.

$$\boldsymbol{z} := \left[\zeta_1, \dot{\zeta}_1, \dots, \zeta_1^{(\beta_1 - 1)}, \dots, \zeta_m, \dots, \zeta_1^{(\beta_m - 1)}\right] \tag{10}$$

The flat input can be obtained from the following :

$$\zeta_i^{(\beta_i)} = \alpha_i\left(\zeta_1, \dot{\zeta}_1, \dots, \zeta_1^{(\beta-1)}, u, \dot{u}, \dots, u^{(\beta_i)}\right) := v_i \tag{11}$$

where the highest derivative β_i of the flat output ζ considered as the new flat input v. For a multi-input flat system:

$$\mathbf{v} := [v_1, v_1, \dots, v_m]^T \tag{12}$$

It is important to note that in Eq. (11), β_i is associated with the relative degree of the system, indicating how the system's outputs respond to the inputs over time. Additionally, the number of flat inputs v_i is determined by the quantity of selected flat outputs ζ_i that effectively represent the nonlinear system. This relationship highlights the connection between the system's structure and its ability to be controlled through flatness.

The standard form can be derived from equations (10) and (12) and is expressed as:

$$\dot{z} = Az + Bv \tag{13}$$

The linear feedback controller v can be obtained as:

$$v = \zeta_d^n - \sum_{i=0}^{n-1} \lambda_i \, e^{n-i-1} \tag{14}$$

where $e = \zeta - \zeta_d$.

The method of feedforward linearization enables trajectory generators or controllers to focus solely on the linear flat model, provided that the initial conditions for both the desired output and the flat output are matched. This approach simplifies the control design process by leveraging the linear characteristics of the flat model while ensuring that the system adheres to the required trajectory. To summarize this discussion, we can conclude the section with the following theorem:

Theorem 1: ([36]) Given a desired trajectory in the flat output ζ_d and a corresponding desired flat input v_d, with the initial condition $z(0) = z_d(0)$, applying the nominal feedforward control law:

$$u = \psi_2(z_d, v_d) \tag{15}$$

To the flat system, as defined in Eq. (4), transforms the system into an equivalent linear representation in Brunovsky canonical form through a suitable change of coordinates. This transformation simplifies the control design by converting the original nonlinear system into a controllable linear model.

B. Active Disturbance Rejection Control

The foundation of active disturbance rejection control is inherited from proportional-integral-derivative (PID), which is an error-driven control law [37]. The main advantages of ADRC are as follows: i) It is robust to the model's uncertainty and exogenous disturbances. ii) Ignores the mathematical model and uses errors when designing the control law. iii) Applicable to a wide range of systems, including flat systems. Constructing the disturbance rejection loop is a crucial step of the ADRC methodology. It facilitates controller design by utilizing the Luenberger observer (LO), which plays an essential role in ADRC by providing an estimate of uncertainty. Using the state observers would allow us to estimate the system's state and total disturbances simultaneously. Using a state observer would reject or compensate for real-time disturbances, leading to an enhancement in the robustness performance of the system. Consider the flat system in matrix form (13) with a perturbed expression:

$$\begin{aligned} \dot{z} &= Az + Bv + E\delta \\ Y &= Cz \end{aligned} \tag{16}$$

where δ can be seen as a disturbance to the system. An expression for LO corresponding to the system (16) can be given as:

$$\dot{\hat{z}} = A\hat{z} + Bv + L\,(Y - C\hat{z}) \tag{17}$$

where L is the observer gain matrix designed to stabilize the error dynamics:

$$\dot{\hat{e}} = (A - LC)\hat{e} + E\delta \tag{18}$$

Asymptotic stability of the dynamics of the estimated error can be achieved when the roots of the matrix $A - LC$ lie in the left half plane. Notting that δ is either constant or directly estimated, and it is bounded for all time t. The disturbance compensator would cancel out the effect of the estimated disturbance on the system. Its function would be to actively compensate for disturbances to achieve robust performance in the face of uncertainties.

C. B-spline design

B-spline is an interpolation technique that estimates unknown values within a range of identified data points, commonly used in fitting, numerical analysis, and data control. B-spline is one of several interpolation methods, such as linear, polynomial, and radial basis function (RBF) interpolation types. In nonlinear control and trajectory generation, the B-spline can generate smooth trajectories. These trajectories can serve as the desired trajectories for flat systems, which impact the performance of the control system design.

A spline provides a function divided into segments; these segments are represented by a polynomial of degree k. Combining all these segments would provide a continuous curve linking specific data points. In addition, incorporating certain numerical values known as knots would enhance the control over the curve's shape. Thus, B-spline functions provide a higher level of mathematical computation than other techniques. These functions can be used in solving boundary control problems due to their strong geometric properties and accuracy in solving spatial domain problems. A B-spline curve can be defined as combining linear control points and basis functions as the following expression:

$$r(t) = \sum_{i=0}^{n} N_{i,k}\,(t)\,P_i \tag{19}$$

where $r(t)$ is the B-spline curve, P_i represents the control points, t is the knot vector parameter, and finally $N_{i,k}(t)$ are the basis functions of degree k.

The knot vector can be defined as: $T = [\,t_0, t_1, \dots, t_m]$ which is an increasing sequence, and the parameter $m = n + k + 1$ ensures the correct choice of basis functions and control points. The value of the curve at each knot determines the influence of each basis function.

The basis spline function $N_{i,k}(t)$ computed as a recursive formula [38], [39], for the k^{th} order basis spline function for $k = 0$:

$$N_{i,0}(t) = \begin{cases} 1, & t_i \le t < t_{i+1} \\ 0, & 0therwise \end{cases} \tag{20}$$

and the recursive formula for the degree k:

$$N_{i,k}(t) = \frac{t - t_i}{t_{i+k} - t_i} N_{i,k-1}(t) + \frac{t_{i+k+1} - t}{t_{i+k+1} - t_{i+1}} N_{i+1,k-1}(t) \tag{21}$$

In (21), the first term accounts for the lower part, while the second term accounts for the upper part of the basis function. To compute B-spline curve derivatives, the basis function is differentiated as:

$$r'(t) = \sum_{i=0}^{n} N'_{i,k}(t)\, P_i \tag{22}$$

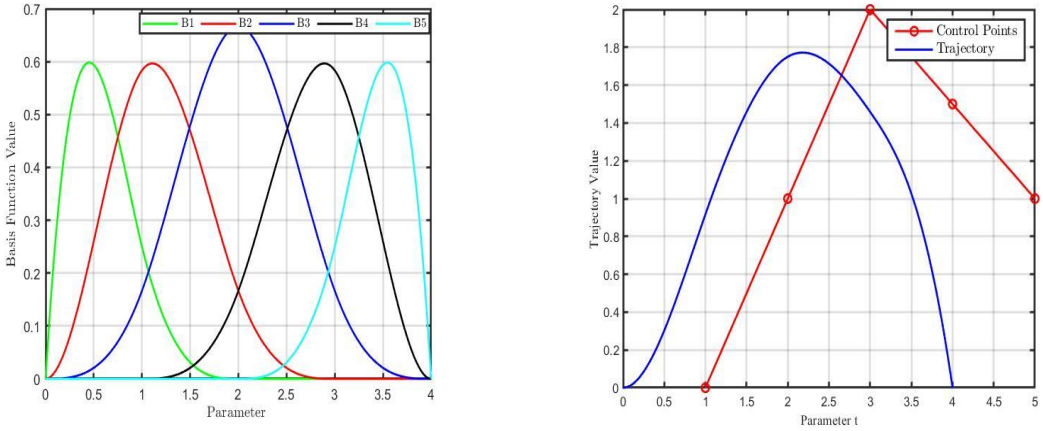

FIG. 3. B-SPLINE (A) BASIS FUNCTION VALUE (B) TRAJECTORY VALUE.

B-spline trajectory generation is an essential feature for designing control systems' trajectories. These trajectories should be differentiable to apply constraints on the first and second derivatives of the B-spline trajectory. Uniform and non-uniform knot vectors can be chosen according to the application requirements. Finally, the order of the B-spline affects the smoothness and computational complexity of the designed curve. In *Fig. 3*, the B-spline basis function and the trajectory values are shown.

IV. FLATNESS-BASED ADRC FOR NCSTR

The nonlinear CSTR system exhibits the property of flatness, meaning it is considered flat if a differential function exists of the states and input, known as the flat output. This flat output allows the system's states and inputs to be expressed as differential functions of the flat output and a finite number of its time derivatives. In the case of a CSTR system, a common scenario involves selecting the reactor temperature $T(t)$ as the controlled output, while the cooling temperature $T_c(t)$ serves as the manipulated variable.

The schematic diagram for the proposed Flatness-based ADRC is presented in *Fig. 4*, consisting of the flatness (2DF) controllers and the disturbance observer. Referring to Eq. (1-2) to facilitate controller design, let $\frac{F}{V} = \alpha$, $\frac{(-\Delta H)}{\rho C_p} = \beta$, and $\frac{UA}{V\rho C_p} = \gamma$.

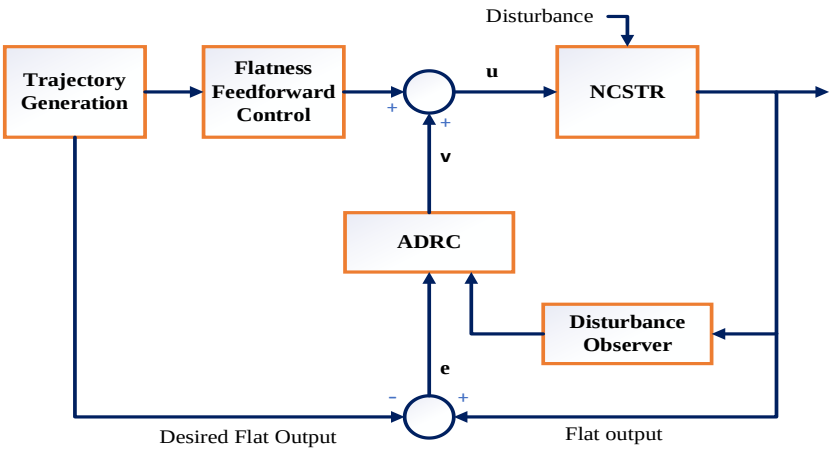

FIG. 4. PROPOSED FLATNESS ADRC SCHEME.

The derivation of the flat system begins by selecting $\zeta(t) = T$ as the flat output. Taking the first derivative of the flat output yields:

$$\dot{\zeta} = \beta k(\zeta)\, \mathsf{C}_A - (\alpha + \gamma)\zeta + \gamma u + \alpha\, T_f \tag{23}$$

The reactor variables and input can be parameterized in terms of the flat output and a finite number of its time derivatives, following the formulation in Eqs. (7) and (8), as:

$$= (1/\beta k(\zeta))\{\dot{\zeta} - \alpha(T_f - \zeta) - \gamma(u - \zeta)\}C_A \tag{24}$$

$$T = \zeta \tag{25}$$

$$u = 1/\gamma\left\{\dot{\zeta} - \beta k(\zeta)c_A + (\alpha + \gamma)\zeta\right\} \tag{26}$$

$$v = \dot{\zeta} \tag{27}$$

The control objective is to force the flat output ζ to track a desired flat output trajectory ζ_d. The error is defined as: $e = \zeta - \zeta_d$ and the error dynamics is: $\dot{e} = \dot{\zeta} - \dot{\zeta_d}$. The dynamics of the flat output can be obtained from Eq. (23) and substituted into the error dynamics, yielding:

$$\dot{e} = \beta k(\zeta)\, \mathsf{C}_A - (\alpha + \gamma)\zeta + \gamma u + \alpha\, T_f - \dot{\zeta_d} \tag{28}$$

Now, by substituting Eq. (26) into (28) to compensate for the value of u, yields:

$$\dot{e} = v + \alpha T_f - \dot{\zeta_d} \tag{29}$$

where αT_f is disturbance input, which is the temperature inlet to the CSTR, and the term will be denoted as d henceforward, and Eq. (29) becomes:

$$\dot{e} = v + d - \dot{\zeta_d} \tag{30}$$

An observer is designed to estimate the disturbance input to the flat system, and we assume that the solution of the observer is the estimated error $\hat{e}$, substitute in the error dynamic Eq. (30) yields:

$$\dot{\hat{e}} = v + \hat{d} \tag{31}$$

where $\hat{d} = L\,\bar{e}$, and $\bar{e} = e - \hat{e}$, this would lead to:

$$\dot{\bar{e}} = d + \hat{d} \tag{32}$$

By assuming that: $\bar{d} = d - \hat{d}$ and since the assumption of constant disturbance implies: $\dot{d} = 0$, which leads to: $\dot{\bar{d}} = -\dot{\hat{d}}$, this would yield the following important relation between the estimated disturbance dynamics and error: $\dot{\hat{d}} = L\dot{\bar{e}}$, then

$$\dot{\bar{d}} = -L\dot{\bar{e}} \tag{33}$$

From Eq. (33), we deduce that: $\dot{\bar{d}} = -L\bar{d}$, this implies that $\bar{d} \to 0 \;\; \forall t \to \infty$. Referring to Eq. (27), we can suggest the feedback control law as:

$$v = -ke - \hat{d} \tag{34}$$

The error dynamics can be obtained by substituting Eq. (30) into Eq. (26) and noting the relation $\bar{d} = d - \hat{d}$, gives the new error dynamics:

$$\dot{e} = -ke + \bar{d} \tag{35}$$

This would imply that, when $\bar{d} \to 0$ results in $e \to 0$ and the flat output will approach the desired flat output: $\zeta \to \zeta_d$.

V. SIMULATION RESULTS

This section presents simulation results to validate the effectiveness of the proposed controller, flatness active disturbance rejection control FADRC. Two reference trajectories are chosen to enhance the overall performance and observation: a switching function (SF) and a B-spline (Bs) curve. B-spline reference trajectories, Bs1 and Bs2, were designed with distinct dynamic response characteristics while ensuring compliance with system constraints. Their design aimed to provide a smooth alternative to the switching function (SF). Meanwhile, maintaining comparable transition dynamics enables a performance comparison regarding tracking accuracy, control effort, and disturbance rejection.

Additionally, the disturbance input in this study corresponds to the inlet temperature of the CSTR, which was perturbed to a constant value of 355 K from its nominal value of 350 K. This perturbation was introduced to assess the system's robustness and the controller's ability to reject disturbances while maintaining desired tracking performance. The controller design parameters for the FADRC are k = 10, L= 10 for the switching function case, and k = 250, L=10 for the B-spline curve.

In the response shown in *Fig. 5*, the FADRC with the disturbance estimator exhibits an overshoot due to the estimator reacting to change and overcompensating while using the SF. In contrast, Bs1 and Bs2 show no overshoot as their smooth transition profiles inherently account for system constraints and mitigate abrupt control actions. Table II lists the performance indexes using the switching function reference input and the B-spline-designed reference trajectories.

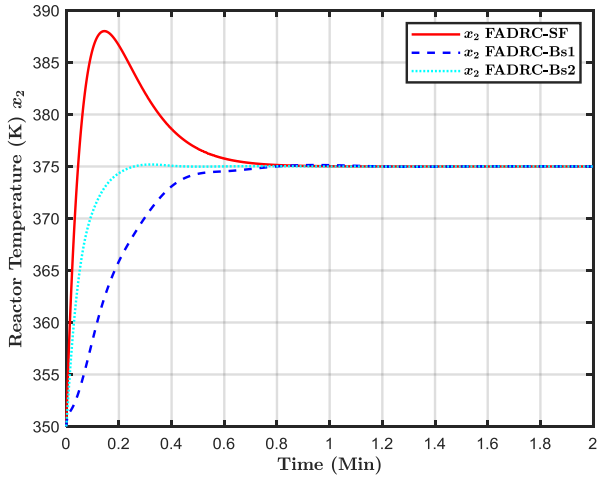

FIG. 5. REACTOR TEMPERATURE TRACKING WITH SWITCHING FUNCTION AND B-SPLINE.

TABLE II. PERFORMANCE INDEXES SWITCHING FUNCTION AND B-SPLINE REFERENCE INPUT

Parameter	RMSE	ITAE	Δu	Overshoot
FADRC-SF	3.1190	0.8736	771.4103	3.47%
FADRC-Bs1	0.1060	0.0233	266.4081	0.04%
FADRC-Bs2	0.1590	0.0229	352.9601	0.05%

As presented in *Fig. 6*, FADRC shows good concentration tracking performance, ensuring accurate concentration regulation while maintaining compatibility with the temperature constraints in the CSTR.

The tracking error for FADRC exhibits a noticeable initial deviation using SF, as shown in *Fig. 7*. Still, the Bs1 and Bs2 errors are minimal after a brief transient period.

The cooling temperature control input for FADRC with the disturbance estimator shows a significant change at the initial step for the SF input and a smoother change with Bs1 and Bs2, as

shown in *Fig. 8*. Constraints were imposed on the control signal to ensure feasible operation, restricting it within the range as $250 \leq u \leq 320$ K.

The control input for the FADRC respected the imposed constraints when using the Bs1 design, while it did not adhere to these constraints when utilizing the switching function (SF) and Bs2 trajectories. The control action follows the smooth trajectory of the B-spline without substantial adjustments, indicating that the ADRC can effectively manage slow and smooth variations in the input signal

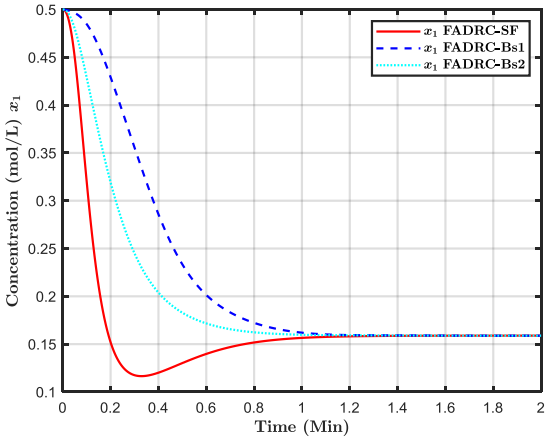

FIG. 6. CONCENTRATION RESPONSE.

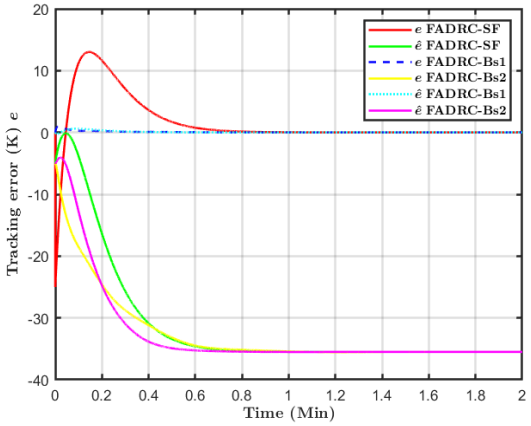

FIG. 7. TRACKING ERROR.

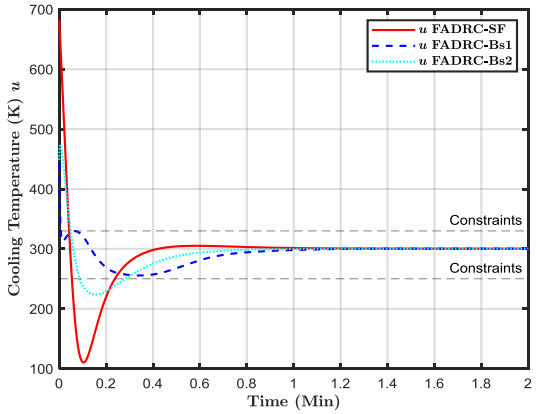

FIG. 8. COOLING TEMPERATURE CONTROL SIGNAL.

In *Fig. 9*, the disturbance estimator in the FADRC reacts promptly to the abrupt disturbance, leading to a more aggressive control action during the transient phase using SF. This results in a higher

initial control effort as the system tries to compensate for the disturbance, which can lead to some overshoot.

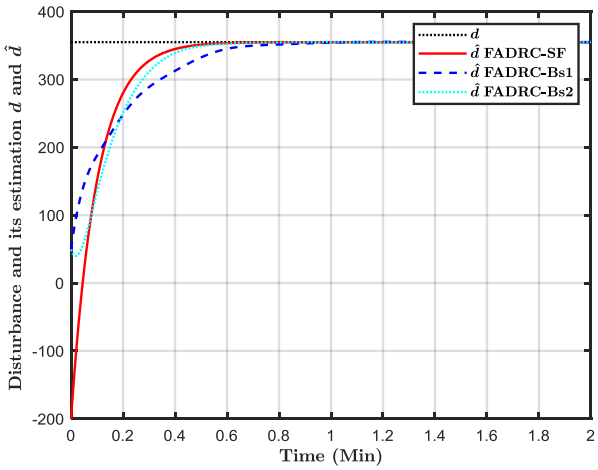

FIG. 9. DISTURBANCE AND ESTIMATION.

The disturbance estimator adapts to the change in the reference, and after the initial compensation, the system quickly settles to the desired value. The estimator's role here is crucial in enabling the system to recover rapidly from disturbances. *Fig. 10* shows the disturbance estimation error for the three presented cases, highlighting the differences between the responses.

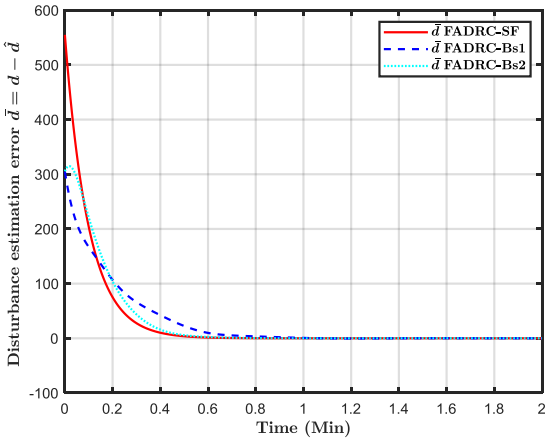

FIG. 10. DISTURBANCE ESTIMATION ERROR.

For the B-spline reference input, the disturbance estimator in the FADRC performs well, gradually adapting to the smooth trajectory. Since the disturbance is more gradual than the switching function, the estimator does not need aggressive corrections, resulting in a more stable and smooth control action. The disturbance estimator ensures precise tracking by compensating for any disturbances in real time. However, the need for significant adjustments is reduced with the B-splines' smoother input.

VI. CONCLUSIONS

The study aims to present a robust control methodology for disturbed CSTR systems. Utilizing the flatness property and flatness-based control. The nonlinear CSTR system was transformed into a normal form, facilitating the design and implementation of a robust feedback controller. FADRC combined state feedback and a disturbance observer technique to estimate the proposed exogenous disturbance on the CSTR. Simulation results were conducted under various reference input trajectories and feed temperature input changes. The tracking performance for the proposed FADRC was investigated and compared. The FADRC effectively references tracking and constraint handling, particularly with the Bs1 trajectory, while exhibiting constraint violations when using the SF and Bs2 trajectories. FADRC, with estimation, improves disturbance rejection. In future studies, the application of FADRC will extend to other chemical processes, such as batch reactors, to further assess the effectiveness of the proposed control strategy.

REFERENCES

[1] Q. M. Hamad and S. M. Raafat, "A Flatness-Based Trajectory Tracking Control for Chemical Reactor," in 2024 21st International Multi-Conference on Systems, Signals & Devices (SSD), Erbil, Iraq: IEEE, Apr. 2024, pp. 819–825. doi: 10.1109/SSD61670.2024.10549742.

[2] Q. M. Hamad and S. M. Raafat, "Flatness-Based Model Predictive Constrained Optimal Control for Chemical Reactor," J. Eur. Systèmes Autom., vol. 57, no. 6, pp. 1583–1592, Dec. 2024, doi: 10.18280/jesa.570605.

[3] Z. Hu, P. Li, and Y. Liu, "Enhancing the Performance of Evolutionary Algorithm by Differential Evolution for Optimizing Distillation Sequence," Molecules, vol. 27, no. 12, p. 3802, Jun. 2022, doi: 10.3390/molecules27123802.

[4] H. Xu, H. S. Ee Chuo, M. K. Tan, C. H. Ng, M. Yang, and K. T. Kin Teo, "Evolutionary Based Control and Optimisation of Exothermic Batch Process," in 2023 IEEE International Conference on Artificial Intelligence in Engineering and Technology (IICAIET), Kota Kinabalu, Malaysia: IEEE, Sep. 2023, pp. 359–364. doi: 10.1109/IICAIET59451.2023.10291909.

[5] M. Herrera, O. Camacho, H. Leiva, and C. Smith, "An approach of dynamic sliding mode control for chemical processes," J. Process Control, vol. 85, pp. 112–120, Jan. 2020, doi: 10.1016/j.jprocont.2019.11.008.

[6] C. Obando, R. Rojas, F. Ulloa, and O. Camacho, "Dual-Mode Based Sliding Mode Control Approach for Nonlinear Chemical Processes," ACS Omega, vol. 8, no. 10, pp. 9511–9525, Mar. 2023, doi: 10.1021/acsomega.2c08201.

[7] M. L. Darby, "Industrial MPC of Continuous Processes," in Encyclopedia of Systems and Control, J. Baillieul and T. Samad, Eds., London: Springer London, 2013, pp. 1–10. doi: 10.1007/978-1-4471-5102-9_242-1.

[8] Z. Wang, W. G. Y. Tan, G. P. Rangaiah, and Z. Wu, "Machine learning aided model predictive control with multi-objective optimization and multi-criteria decision making," Comput. Chem. Eng., vol. 179, p. 108414, Nov. 2023, doi: 10.1016/j.compchemeng.2023.108414.

[9] Z. Wu, A. Alnajdi, Q. Gu, and P. D. Christofides, "Statistical machine- learning– based predictive control of uncertain nonlinear processes," AIChE J., vol. 68, no. 5, p. e17642, May 2022, doi: 10.1002/aic.17642.

[10] M. Ouyang and Y. Wang, "Optimization and Realization of the Continuous Reactor with Improved Automatic Disturbance Rejection Control," Complexity, vol. 2020, pp. 1–14, Nov. 2020, doi: 10.1155/2020/4519428.

[11] D. Das, S. Chakraborty, and A. K. Naskar, "Controller design on a new 2DOF PID structure for different processes having integrating nature for both the step and ramp type of signals," Int. J. Syst. Sci., vol. 54, no. 7, pp. 1423–1450, May 2023, doi: 10.1080/00207721.2023.2177903.

[12] W. L. Luyben, "Comparison of additive and multiplicative feedforward control," J. Process Control, vol. 111, pp. 1–7, Mar. 2022, doi: 10.1016/j.jprocont.2022.01.004.

[13] D. Das, S. Chakraborty, and G. L. Raja, "Enhanced dual-DOF PI-PD control of integrating-type chemical processes," Int. J. Chem. React. Eng., vol. 21, no. 7, pp. 907–920, Jul. 2023, doi: 10.1515/ijcre-2022-0156.

[14] N. Ahmed Alawad, A. Jaleel Humaidi, and A. Sabah Alaraji, "Modified Tracking Differentiator for Enhancing the Performance of Exoskeleton Knee System Based on Active Disturbance Rejection Control," Iraqi J. Comput. Commun. Control Syst. Eng., pp. 69–83, Mar. 2023, doi: 10.33103/uot.ijccce.23.1.6.

[15] N. Ahmed Alawad, A. Jaleel Humaidi, and A. Sabah Alaraji, "Fractional proportional derivative-based active disturbance rejection control of knee exoskeleton device for rehabilitation care," Indones. J. Electr. Eng. Comput. Sci., vol. 28, no. 3, p. 1405, Dec. 2022, doi: 10.11591/ijeecs.v28.i3.pp1405-1413.

[16] W. Wei, N. Chen, Z. Zhang, Z. Liu, and M. Zuo, "U-Model-Based Active Disturbance Rejection Control for the Dissolved Oxygen in a Wastewater Treatment Process," Math. Probl. Eng., vol. 2020, pp. 1–14, May 2020, doi: 10.1155/2020/3507910.

[17] T. He, Z. Wu, D. Li, and J. Wang, "A Tuning Method of Active Disturbance Rejection Control for a Class of High-Order Processes," IEEE Trans. Ind. Electron., vol. 67, no. 4, pp. 3191–3201, Apr. 2020, doi: 10.1109/TIE.2019.2908592.

[18] W. Xue and B. Xin, "Active disturbance rejection control: Practical technology and industrial application," Adv. Control Appl., vol. 3, no. 2, p. e91, Jun. 2021, doi: 10.1002/adc2.91.

[19] H. Sira-Ramírez and E. W. Zurita-Bustamante, "On the equivalence between ADRC and Flat Filter based controllers: A frequency domain approach," Control Eng. Pract., vol. 107, p. 104656, Feb. 2021, doi: 10.1016/j.conengprac.2020.104656.

[20] Z.-H. Wu, F. Deng, B.-Z. Guo, C. Wu, and Q. Xiang, "Backstepping Active Disturbance Rejection Control for Lower Triangular Nonlinear Systems With Mismatched Stochastic Disturbances," IEEE Trans. Syst. Man Cybern. Syst., vol. 52, no. 4, pp. 2688–2702, Apr. 2022, doi: 10.1109/TSMC.2021.3050820.

[21] Y. Huang and J. Su, "Output feedback stabilization of uncertain nonholonomic systems with external disturbances via active disturbance rejection control," ISA Trans., vol. 104, pp. 245–254, Sep. 2020, doi: 10.1016/j.isatra.2020.05.009.

[22] M. R. Stanković, R. Madonski, S. Shao, and D. Mikluc, "On dealing with harmonic uncertainties in the class of active disturbance rejection controllers," Int. J. Control, vol. 94, no. 10, pp. 2795–2810, Oct. 2021, doi: 10.1080/00207179.2020.1736639.

[23] A. H. Hameed, S. A. Al-Samarraie, and A. J. Humaidi, "Backstepping-based nonlinear disturbance observer for speed control of DC motor," presented at the THE FIFTH SCIENTIFIC CONFERENCE FOR ELECTRICAL ENGINEERING TECHNIQUES RESEARCH (EETR2024), Baghdad, Iraq, 2024, p. 030007. doi: 10.1063/5.0236229.

[24] A. H. Hameed, S. A. Al-Samarraie, A. J. Humaidi, and N. Saeed, "Backstepping-Based Quasi-Sliding Mode Control and Observation for Electric Vehicle Systems: A Solution to Unmatched Load and Road Perturbations," World Electr. Veh. J., vol. 15, no. 9, p. 419, Sep. 2024, doi: 10.3390/wevj15090419.

[25] A. H. Hameed, S. A. Al-Samarraie, A. J. Humaidi, "A Comparative Study of Flux Observers in Induction Motors," Iraqi J. Comput. Commun. Control Syst. Eng., pp. 103–118, Mar. 2024, doi: 10.33103/uot.ijccce.24.1.8.

[26] N. Gu, D. Wang, Z. Peng, J. Wang, and Q.-L. Han, "Disturbance observers and extended state observers for marine vehicles: A survey," Control Eng. Pract., vol. 123, p. 105158, Jun. 2022, doi: 10.1016/j.conengprac.2022.105158.

[27] R. Wang and J. Shen, "Disturbance Observer and Adaptive Control for Disturbance Rejection of Quadrotor: A Survey," Actuators, vol. 13, no. 6, p. 217, Jun. 2024, doi: 10.3390/act13060217.

[28] S. Ahmad and A. Ali, "Unified Disturbance-Estimation-Based Control and Equivalence With IMC and PID: Case Study on a DC–DC Boost Converter," IEEE Trans. Ind. Electron., vol. 68, no. 6, pp. 5122–5132, Jun. 2021, doi: 10.1109/TIE.2020.2987269.

[29] A. Bayrak, B. Kurkcu, and M. O. Efe, "A New Adaptive Disturbance/Uncertainty Estimator Based Control Scheme For LTI Systems," IEEE Access, vol. 10, pp. 106849–106858, 2022, doi: 10.1109/ACCESS.2022.3209346.

[30] L. Biagiotti, L. Moriello, and C. Melchiorri, "Improving the Accuracy of Industrial Robots via Iterative Reference Trajectory Modification," IEEE Trans. Control Syst. Technol., vol. 28, no. 3, pp. 831–843, May 2020, doi: 10.1109/TCST.2019.2892929.

[31] A. Dumanli and B. Sencer, "Robust Trajectory Generation for Multi-Axis Vibration Avoidance," IEEEASME Trans. Mechatron., pp. 1–1, 2020, doi: 10.1109/TMECH.2020.2999743.

[32] X. Li, X. Gao, W. Zhang, and L. Hao, "Smooth and collision-free trajectory generation in cluttered environments using cubic B-spline form," Mech. Mach. Theory, vol. 169, p. 104606, Mar. 2022, doi: 10.1016/j.mechmachtheory.2021.104606.

[33] R. vanHoek, J. Ploeg, and H. Nijmeijer, "Cooperative Driving of Automated Vehicles Using B-Splines for Trajectory Planning," IEEE Trans. Intell. Veh., vol. 6, no. 3, pp. 594–604, Sep. 2021, doi: 10.1109/TIV.2021.3072679.

[34] H. Sira-Ramírez, Differentially Flat Systems, 1st ed. CRC Press, 2004. doi: 10.1201/9781482276640.

[35] M. Fliess, J. Lévine, P. Martin, and P. Rouchon, "Flatness and defect of non-linear systems: introductory theory and examples," Int. J. Control, vol. 61, no. 6, pp. 1327–1361, Jun. 1995, doi: 10.1080/00207179508921959.

[36] C. Huang and H. Sira-Ramírez, "Flatness-based active disturbance rejection control for linear systems with unknown time-varying coefficients," Int. J. Control, vol. 88, no. 12, pp. 2578–2587, Dec. 2015, doi: 10.1080/00207179.2015.1050699.

[37] G. Herbst and R. Madonski, Active Disturbance Rejection Control: From Principles to Practice. in Control Engineering. Cham: Springer Nature Switzerland, 2025. doi: 10.1007/978-3-031-72687-3.

[38] C. De Boor, "On calculating with B-splines," J. Approx. Theory, vol. 6, no. 1, pp. 50–62, Jul. 1972, doi: 10.1016/0021-9045(72)90080-9.

[39] J. R. and C. De Boor, "A Practical Guide to Splines.," Math. Comput., vol. 34, no. 149, p. 325, Jan. 1980, doi: 10.2307/2006241.